Journal of Cerebral Blood Flow & Metabolism (2010) 30, 1767–1776

www.jcbfm.com

Cerebellum as the normal reference for the detection of increased cerebral oxygen extraction

Thomas T Jiang[1], Tom O Videen[1,2], Robert L Grubb Jr[1,3], William J Powers[4] and Colin P Derdeyn[1,2,3]

[1]*Mallinckrodt Institute of Radiology, Washington University School of Medicine, St Louis, Missouri, USA;* [2]*Department of Neurology, Washington University School of Medicine, St Louis, Missouri, USA;* [3]*Department of Neurological Surgery, Washington University School of Medicine, St Louis, Missouri, USA;* [4]*Department of Neurology, University of North Carolina, Chapel Hill, North Carolina, USA*

Hemispheric ratios of oxygen extraction fraction (OEF), a proven methodology for the detection of severe hemodynamic impairment and stroke risk, are not sensitive for detecting bilateral hemispheric increases in OEF. The aim of this study was to investigate the use of cerebellum as the reference normal. We analyzed positron emission tomographic (PET) measurements of count-based OEF and clinical data from 57 patients with unilateral atherosclerotic carotid occlusion and 13 controls enrolled in a prospective study of stroke risk. The ipsilateral, contralateral, and total cerebellum were each evaluated as possible reference regions, and the ratios of the middle cerebral artery (MCA) hemispheric OEF counts against those in each reference region were determined. A statistically significant correlation (*$P<0.0001$*) was observed with all three MCA-to-cerebellar ratios when compared with the gold standard of ipsilateral-to-contralateral MCA hemispheric ratio. Kaplan–Meier analyses showed all MCA-to-cerebellar ratios to be predictive of stroke. By using the total cerebellum method, 7 strokes were found to have occurred in 20 patients with increased OEF (*$P=0.0007$*), compared with 7 strokes out of 16 patients with elevated OEF using the ipsilateral or contralateral cerebellum methods (*$P<0.0001$*). These methods may be useful for categorizing the hemodynamic status of patients with bilateral cerebral occlusive diseases, including atherosclerosis and moyamoya, to determine the association with the risk of subsequent stroke.
Journal of Cerebral Blood Flow & Metabolism (2010) **30,** 1767–1776; doi:10.1038/jcbfm.2010.43; published online 7 April 2010

Keywords: oxygen extraction fraction; PET; stroke

Introduction

Misery perfusion constitutes a hemodynamic state in which cerebral blood flow (CBF) falls, yet oxygen metabolism is maintained by increased oxygen extraction fraction (OEF) (Baron *et al*, 1981). Increased OEF can be measured using positron emission tomography (PET) and is a powerful predictor of subsequent ischemic stroke in patients with atherosclerotic carotid artery disease (Grubb *et al*, 1998; Yamauchi *et al*, 1999).

Several methods for measuring OEF have been developed. The steady-state method with inhalation of ^{15}O-labeled gas (Frackowiak *et al*, 1980) and the bolus method with bolus injection of ^{15}O-labeled water (Mintun *et al*, 1984) both require arterial blood sampling during PET studies to convert PET counts into quantitative OEF measurements. However, arterial blood sampling is an invasive procedure, and percutaneous arterial cannulation may not be possible in all patients (Grubb *et al*, 1998). In addition, the quantitative processing of OEF images requires considerable technical expertise. For these reasons, a count-based method using a ratio of the counts from separate ^{15}O-labeled oxygen and ^{15}O-labeled water scans can be used (Derdeyn *et al*, 1999; Jones *et al*, 1976; Kobayashi *et al*, 2006). The count-based OEF (cbOEF) methods correlate well with the quantitative techniques (Derdeyn *et al*, 2001, 1999; Kobayashi *et al*, 2006), though a correction for cerebral blood volume (CBV) has been shown to be beneficial when measuring cbOEF using the steady-state method (but unnecessary for the bolus method) (Derdeyn *et al*, 2001, 1999; Kobayashi *et al*, 2006). Recent advancements in the count-based method have reduced the examination time and exposure to radioactive gas (Derdeyn *et al*, 2001, 1999; Kobayashi *et al*, 2006).

Correspondence: Dr CP Derdeyn, Department of Neurological Surgery, Washington University School of Medicine, 510 South Kingshighway Blvd., St Louis, MO 63110, USA.
E-mail: derdeync@wustl.edu
This study was supported by NIH grants NS28947, NS02029, NS 051631, NS42167, and a Radiological Society of North America/Siemens Medical Systems Research Fellowship.
Received 23 December 2009; revised 2 March 2010; accepted 3 March 2010; published online 7 April 2010

In earlier studies, subjects have been defined as normal or abnormal based on absolute values of OEF (Yamauchi *et al*, 1999), or by comparing quantitative or nonquantitative (count-based) OEF values from the affected hemisphere to identical regions in the unaffected hemisphere (ratios) (Grubb *et al*, 1998; Kobayashi *et al*, 2006; Yamauchi *et al*, 1999). The count-based method, as it does not involve quantitative assessment of OEF, must be analyzed as an asymmetry against a normal reference region. In diseases that involve both carotid territories, such as bilateral atherosclerotic carotid occlusion or the moyamoya phenomenon, the latter method of comparing hemispheric values will not detect a bilateral increase in OEF.

The cerebellum has been used as the reference region in earlier studies, but this method has not been validated as a predictor of stroke risk (Ibaraki *et al*, 2004; Imaizumi *et al*, 2002; Tanaka *et al*, 2006). A major potential limitation of this technique is the phenomenon of crossed cerebellar diaschisis (CCD), a functional reduction in metabolism and blood flow in the cerebellar hemisphere contralateral to an ischemic stroke of the frontal or temporal lobes (Feeney and Baron, 1986; Pantano *et al*, 1986; Yamauchi *et al*, 1992). In addition to an asymmetry in metabolism and flow between the two cerebellar hemispheres, CCD may lead to an increase in OEF in the affected cerebellar hemisphere, owing to a greater reduction in flow than oxygen metabolism (Yamauchi *et al*, 1992). However, this phenomenon has not been consistently identified (Pantano *et al*, 1986).

The aim of this study was to determine whether the cerebellum could be used as the reference normal for a hemispheric increase in OEF. We analyzed the data from a prospective study of OEF as a predictor of stroke risk in atherosclerotic carotid occlusion (the St Louis Carotid Occlusion Study, STLCOS; Grubb *et al*, 1998), using the count-based method and the cerebellum as the normal reference.

Materials and methods

This study was a retrospective analysis of prospectively collected clinical and PET data from 57 patients with symptomatic atherosclerotic carotid artery occlusion and 13 normal control subjects enrolled in the STLCOS (Grubb *et al*, 1998). All patients had unilateral atherosclerotic occlusion of the common or internal carotid arteries and ipsilateral ischemic symptoms. Patients were followed up for the occurrence of stroke or death during the course of the study, resulting in a mean follow-up of 29.5 months with a range of 6.2 to 61.9 months. All studies were performed under institutional review board-approved protocols. Informed consent was obtained from all subjects.

Subjects

Eighty-one patients with unilateral symptomatic atherosclerotic carotid arterial occlusion were enrolled in the STLCOS, which is a blinded prospective study of cerebral hemodynamics and ischemic stroke. Owing to the technical issues discussed below, the data from only 57 of the 81 patients were used for this analysis. The study was designed to test the hypothesis that increased OEF measured in the cerebral hemisphere distal to the occluded carotid artery was an independent predictor of stroke in these patients. Analysis of both the baseline risk factors and of the long-term follow-up has been reported earlier (Derdeyn *et al*, 1998; Grubb *et al*, 1998). Details of the study design, patient population, and inclusion and exclusion criteria can be found in these two reports. The primary end point of the original prospective study was subsequent ischemic stroke, defined clinically as a neurologic deficit of presumed ischemic cerebrovascular cause lasting >24 hours in any cerebrovascular territory.

Eighteen healthy control subjects (8 women, 10 men; mean age $\pm$ s.d., 45 ± 18) were recruited by means of public advertisement. All underwent neurologic evaluation, magnetic resonance (MR) imaging of the head, and duplex ultrasonographic imaging of the extracranial carotid arteries. None had (1) signs or symptoms of neurologic disease other than mild distal sensory loss in the legs consistent with age, (2) pathologic lesions on MR images (mild atrophy and punctate asymptomatic white matter abnormalities were not considered pathologic), or (3) $>50\%$ stenosis of the extracranial carotid arteries.

Positron Emission Tomography Examination

Twenty-four patients recruited into STLCOS were excluded from this analysis, as the smaller axial field of view (FOV) of the initial PET scanner (ECAT 953B, Siemens/CTI, Knoxville, TN, USA) used for this study did not include a sufficient volume of the cerebellum. If the volume of cerebellum included in the scan was $<50\%$ of the total cerebellar volume (based on the atlas described below), those patients were excluded. Thirty-three patients studied on this scanner had an adequate amount of cerebellum and were included in this analysis. The remaining 24 of the 57 STLCOS patients included in this analysis were studied consecutively on an ECAT EXACT HR (Siemens/CTI) with a larger axial FOV. The PET studies of only 13 of the original 18 normal controls could be identified. The PET studies were performed at study entry. After positioning the patient in the scanner gantry, an individually molded thermoplastic facemask was applied to ensure that the patient's head remained in a constant position during the scanning period. Venous and, when possible, arterial catheters were placed for intravenous administration of the radiotracer and for arterial blood gas analyses and arterial time–activity curve determination. All PET scans were acquired in two-dimensional (2D) mode (interslice septa extended). A transmission scan was obtained before radiotracer administration by using Ge-68/Ga-68 rotating rod sources.

A 40-second scan was obtained after inhalation of 1 to 2 breaths of air containing $\sim$100 mCi of ^{15}O-labeled oxygen in trace amounts. After 15 minutes, a second scan was acquired after the bolus injection of $\sim$75 mCi of

^{15}O-labeled water. Specific details regarding the PET acquisition of these scans have been reported in an earlier publication (Derdeyn *et al*, 1999). All radionuclides were produced in the Washington University cyclotron facility (Welch *et al*, 1969; Welch and Ter-Pogossian, 1968).

Image Processing and Analysis

All images were reconstructed by using filtered back-projection and scatter correction with a ramp filter at the Nyquist frequency. They were then filtered with a three-dimensional Gaussian filter to a uniform resolution of 10 mm full-width at half-maximum. These images were subsequently transformed to stereotactic atlas space using a nine-parameter fit (Talairach and Tournoux, 1988; Woods *et al*, 1992; Woods *et al*, 1998). In 14 patients, the automated transformation into stereotactic atlas space failed (due to insufficient sampling of the brain) and required manual transformation using an interactive nine-parameter approach. The atlas transformation permits reproducible placement of regions of interest (ROIs). A cbOEF image was then generated as the normalized ratio image of the counts in the filtered and atlas-transformed ^{15}O-labeled oxygen and ^{15}O-labeled water images, a process that had been reported earlier (Derdeyn *et al*, 1999).

For each patient and control, a large ROI was placed in the territory of the middle cerebral artery (MCA) in each hemisphere, based on a conservative estimate of the vessel's anatomical distribution (Figure 1) (van der Zwan *et al*, 1992). This included gray and white matter and was placed by using stereotactic atlas outlines. Areas of prior infarction identified on the ^{15}O-labeled oxygen images were omitted by hand drawing the boundaries of the infarct and then mirroring the excluded region in the contralateral hemisphere. This method (termed the MCA_{core} method) differed from our earlier work, in which seven 17-mm spheres were placed in the MCA territory by stereotactic coordinates (termed the MCA_{sphere} method) (Fox *et al*, 1985). Using this new method, 200 cm^3 of the MCA territory was sampled per patient.

Cerebellar regions were similarly placed bilaterally using atlas outlines and carefully drawn to exclude the venous sinuses surrounding the cerebellum (Figure 1, arrow). These cerebellar regions were then visually inspected for each patient, and in two instances where the cerebellar ROIs impinged onto the adjacent venous sinuses the ROIs were manually redrawn to exclude these sinuses. The redrawn ROIs were stereotactically placed to ensure left-to-right symmetry. Total cerebellar counts were obtained by adding both ROIs. Cerebellar counts were categorized as being total or ipsilateral or contralateral relative to the symptomatic carotid occlusion. A total of 60 cm^3 of cerebellum was sampled per patient.

Ratios of ipsilateral-to-contralateral MCA territory cbOEF were generated using the original seven-sphere method (MCA_{sphere}) and the large contiguous region (MCA_{core}). Ratios of ipsilateral MCA_{core}-to-cerebellar cbOEF were generated for the entire cerebellum ($cerebellum_{total}$), the ipsilateral cerebellum ($cerebellum_{ipsi}$), and the contralateral cerebellum ($cerebellum_{contra}$).

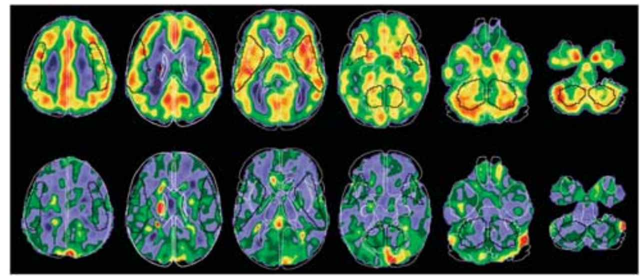

Figure 1 Both the cerebral blood flow positron emission tomography (PET) image (top row) and the oxygen extraction fraction (OEF) PET image (bottom row) were transformed into stereotactic atlas space to allow placement of large MCA_{core} and cerebellar regions of interest. Note the high signal on the OEF image corresponding to venous sinuses surrounding the cerebellum (arrow). These images were created using a 10-mm filter for the purpose of regional analysis. Abbreviation: MCA, middle cerebral artery.

Data Analysis

First, we performed linear regression and Bland–Altman analyses comparing ipsilateral-to-contralateral MCA cbOEF ratios from the MCA_{sphere} to MCA_{core} methods to investigate the correspondence of the original sphere method to the new regional method. Then, we evaluated the MCA_{sphere} cbOEF ratios versus the ratios of the ipsilateral MCA_{core}-to-$cerebellum_{ipsi}$, $cerebellum_{contra}$, and $cerebellum_{total}$, respectively.

Next, we tested the ability of the MCA/cerebellar cbOEF ratios to predict subsequent stroke. The 57 patients were divided into two groups based on the 95% confidence limits (CLs) for the range of cbOEF ratios obtained from the 13 controls: those with abnormal cbOEF ratios and those with normal ratios. We used the 95% CLs rather than the range observed in the normal controls because of our smaller sample size, as well as the widespread acceptance of the use of 95% CLs (Derdeyn *et al*, 2002; Yamauchi *et al*, 1999). We examined the number of patients that changed categories (normal versus abnormal) for each method compared with the ipsilateral-to-contralateral cbOEF MCA_{sphere} categorization. Finally, the primary analysis compared the two groups with respect to the length of time taken before reaching the end point of ipsilateral stroke by means of Kaplan–Meier survival curves and the log-rank statistic.

The presence of CCD was determined from analysis of the ^{15}O-labeled water scans. The regions created on the cbOEF images described above were placed on the ^{15}O-labeled water studies for all patients and normal controls. The 95% CLs for the left-to-right cerebellar CBF were determined from the 13 normal control subjects. Patients with left-sided carotid occlusion were evaluated using the lower limit of the right-to-left cerebellar CBF 95% CL and the reciprocal of the upper limit for right-sided occlusion owing to the baseline normal left/right asymmetry. Values that fell outside these limits were considered to have PET evidence of diaschisis.

We compared the ipsilateral-to-contralateral cerebellar cbOEF ratios between the patients with and without CCD to determine whether there was a significant increase in OEF in the contralateral cerebellum of patients with CCD (Student's *t* test). We also examined the number of patients with CCD that changed categorization. We compared 16 baseline epidemiological, clinical, and laboratory stroke risk factors between this group with CCD and those without. Student's *t* tests, χ^2, and Fisher exact tests were used to assess the statistical significance ($P<0.05$). Because of the multiple comparisons involved in the analyses, a Bonferroni correction was applied to the significance level to maintain the overall type I error rate at 0.05. A total of 16 separate comparisons were made, and therefore the probability value required to accept statistical significance was 0.05/16 or 0.003.

Results

Linear Regression and Bland–Altman Analysis

The results of the linear regression and Bland–Atlman analyses are shown in Figure 2. Ipsilateral/contralateral MCA_{core} cbOEF ratios had a strong correlation with ipsilateral/contralateral MCA_{sphere} cbOEF ratios ($R^2=0.76$, $P<0.0001$). $Cerebellum_{total}$, $cerebellum_{ipsi}$, and $cerebellum_{contra}$ all correlated well with MCA_{sphere} ($R^2=0.59$, 0.59, and 0.52, respectively, $P<0.0001$). The bias was lowest for the MCA_{core} method (0.009), with the $cerebellum_{total}$, $cerebellum_{ipsi}$, and $cerebellum_{contra}$ methods having comparable biases (0.020, 0.018, and 0.020, respectively).

95% Confidence Limits

95% Confidence limits for MCA_{core}, $cerebellum_{total}$, $cerebellum_{ipsi}$, and $cerebellum_{contra}$ ratios were compiled from 13 healthy control subjects and are presented in Table 1. The normal range for MCA_{sphere} was previously reported to be 0.935 to 1.062 (Derdeyn *et al*, 1999), very similar to the MCA_{core} range of 0.945 to 1.061 observed in the present analysis. $Cerebellum_{total}$ had the narrowest CLs (0.858 to 1.099), followed by $cerebellum_{contra}$ and $cerebellum_{ipsi}$ (0.850 to 1.107 and 0.845 to 1.113, respectively). A left-to-right cerebellar cbOEF ratio was also included to evaluate cerebellar symmetry. The mean ± s.d. for left-to-right cerebellum cbOEF ratio was 0.98 ± 0.044 ($P>0.05$).

Categorization

A summary of patient categorization as having normal or elevated OEF can be found in Figure 3 (numbers in blue at each time point denote patients with normal OEF, whereas numbers in red denote those with elevated OEF). A summary of patients who changed their cbOEF status (normal or increased) using each method is presented in Table 2. For example, four patients who were outside of the normal range using MCA_{sphere} were within the normal range using MCA_{core}, whereas four patients within the normal range using MCA_{sphere} were outside of the normal range using MCA_{core}. None of the patients who suffered a stroke during follow-up switched cbOEF status.

Prediction of Stroke Risk

Eight out of 57 STLCOS subjects suffered strokes ipsilateral to their carotid occlusion, during a mean follow-up period of 2.3 years. Using the MCA_{sphere} method with these 57 patients and 13 normal controls, 27 had abnormal cbOEF ratios. All abnormal ratios were ipsilateral to the occluded symptomatic carotid artery and were increased, falling outside the upper limit of normal. Seven patients with ipsilateral stroke during follow-up had increased cbOEF. The remaining 30 patients had normal cbOEF ratios, of whom one suffered a stroke. This analysis was repeated for each of the three MCA_{core}-to-cerebellar cbOEF ratios. All methods were shown to be significant as predictors of stroke risk. The Kaplan–Meier cumulative hazard curve for each method is shown in Figure 3.

Diaschisis

The 95% CLs for left/right and right/left cerebellar cbCBF were 0.959 to 1.056 and 0.946 to 1.04, respectively. In all, 14 of the 57 subjects had ratios outside this range (Table 3). All demonstrated reduced CBF in the cerebellar hemisphere contralateral to the carotid occlusion, consistent with CCD. The OEF tended to be higher in the cerebellar hemisphere with the reduced CBF, but this difference was not statistically significant when compared with the group without diaschisis ($P=0.10$) or the normal controls ($P=0.31$). Four of the patients with diaschisis suffered strokes during follow-up. All four were categorized as abnormal by each of the MCA-to-MCA and MCA-to-cerebellar ratio methods.

Baseline stroke risk factors, demographic and clinical information for the 57 patients as a group, as well as for the 14 patients with CCD are shown in Table 4. Patients with CCD were more likely to have presented with stroke (12 of 14) as compared with those without CCD (21 of 43). The two CCD patients without stroke had a history of transient ischemic attack. Current smokers were more likely to have CCD.

Contralateral Occlusive Disease

Seven patients had >50% stenosis of the contralateral carotid artery. There were no patients with bilateral carotid occlusion. A subanalysis of this small group reveals only one patient with abnormal hemispheric-to-cerebellar OEF ratios, which were

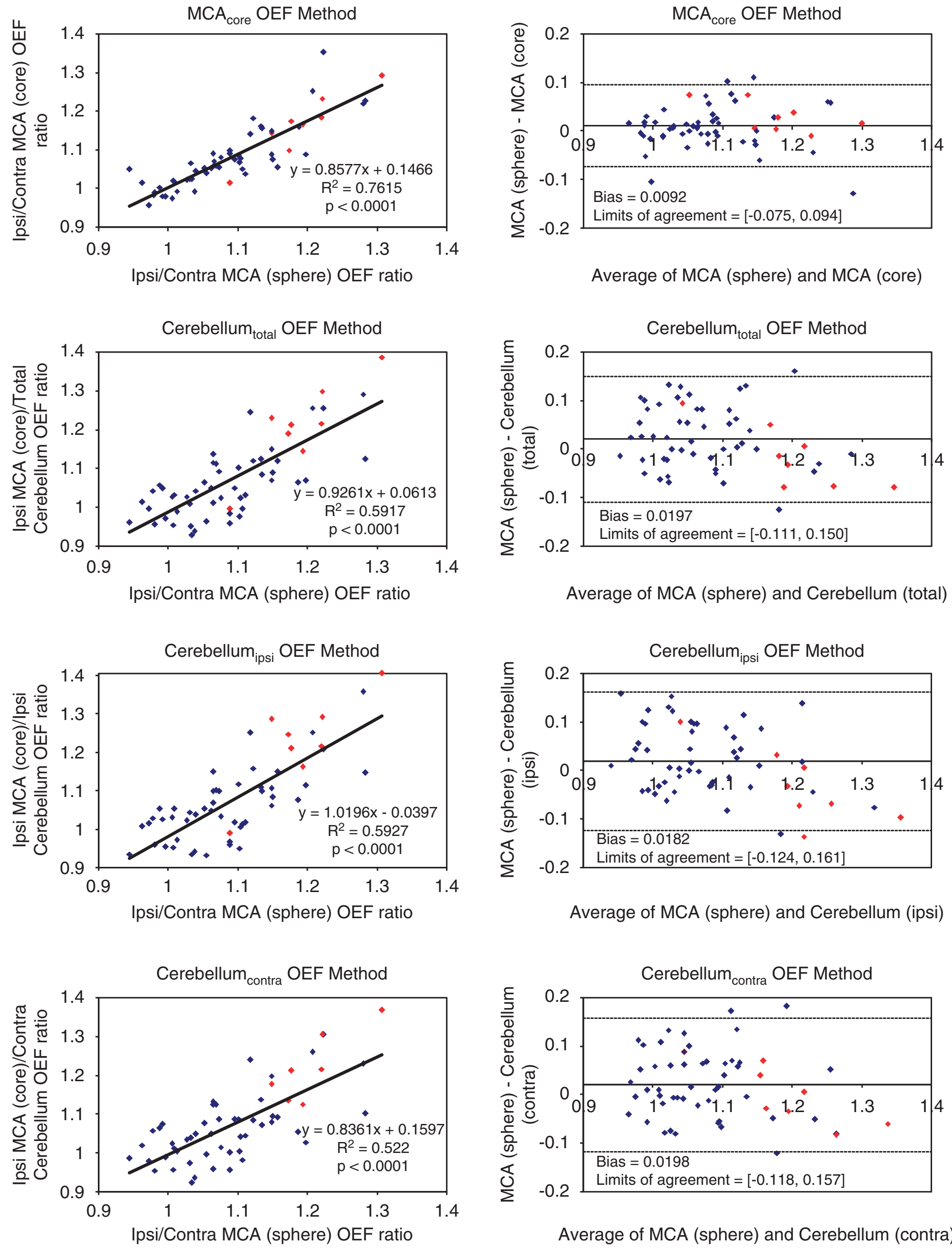

Figure 2 Linear regression analyses (left column) showe a significant correlation between ipsilateral-to-contralateral hemispheric OEF ratios obtained using the MCA_{core} method and those obtained using the MCA_{sphere} method. Similarly, significant correlations between each of the cerebellar methods and the MCA_{sphere} method were found. Bland–Altman analyses (right column) show no systemic biases, with all ratios generally clustering around zero, and a similar, small, number of outliers above and below the limits. Data points highlighted in red represent patients who suffered an ipsilateral stroke during follow-up. Patients with stroke on follow-up tended to have the highest elevations of OEF on all ratio methods. Abbreviations: MCA, middle cerebral artery; OEF, oxygen extraction fraction.

consistently elevated regardless of which cerebellar method was used. This was the only patient to develop subsequent stroke. The other six patients had normal hemispheric-to-cerebellar OEF ratios. However, one of these six patients had an elevated MCA_{sphere} OEF ratio. The same patient, along with another of the six nonstroke patients, also had an elevated MCA_{core} OEF ratio. Linear regression analyses (not shown) showed good correlations between MCA_{sphere} OEF ratios and MCA_{core} ($R^2=0.95$), $cerebellum_{total}$ ($R^2=0.64$), $cerebellum_{ipsi}$ ($R^2=0.60$), and $cerebellum_{contra}$ ($R^2=0.64$), respectively.

Table 1 95% Confidence limits of normal cbOEF ratios ($n = 13$)

	Mean	*s.d.*	*95% CL*
Ipsi/contra MCA_{sphere}	1.008	0.037	0.927, 1.090
Ipsi/contra MCA_{core}	1.002	0.033	0.930, 1.074
Ipsi MCA_{core}/$cerebellum_{total}$	0.978	0.058	0.858, 1.099
Ipsi MCA_{core}/$cerebellum_{ipsi}$	0.979	0.065	0.845, 1.113
Ipsi MCA_{core}/$cerebellum_{contra}$	0.979	0.062	0.850, 1.107

Abbreviations: cbOEF, count-based oxygen extraction fraction; CL, confidence limit; MCA, middle cerebral artery.

Discussion

The cerebellum performed well as the reference normal for identifying increased hemispheric cbOEF. Ratios of hemisphere to cerebellar cbOEF were powerfully predictive of stroke risk. The total and ipsilateral cerebellum performed slightly better than the contralateral cerebellum, which is likely a result of CCD. This technique may be useful in the evaluation of patients with bilateral anterior circulation occlusive processes such as the moyamoya phenomenon.

The count-based methods have a number of advantages over quantitative techniques. Arterial access is not always possible in some patients. Count-based studies do not require arterial sampling and do not require complex metabolic processing. Unlike quantitative OEF studies, count-based methods do not require a correction for intravascular ^{15}O-labeled oxygen, making them easier to process. In our prior comparisons of the count-based hemispheric ratio with the hemispheric ratio of quantitative OEF and absolute quantitative OEF, the hemispheric cbOEF was more accurate in predicting stroke risk (Derdeyn *et al*, 2001, 1999). It is not clear whether this is because of errors in the quantitative OEF calculations, variability in OEF between subjects, or perhaps the effect of uncorrected CBV leading to a more sensitive identification of misery perfusion with the cbOEF method. Regarding variability in OEF between subjects, for example, a hemispheric OEF of 40% may be normal for one person and increased for another. The hemispheric ratios account for this.

In this study, we used a single large ROI, rather than discrete spheres, for the regional analyses of these images (Derdeyn *et al*, 2001, 1999). We created a conservative map of the middle cerebral territory based on the studies of van der Zwan *et al* (1992). One reason for the use of these larger, contiguous regions was for patients with MCA territory infarction. In the sphere method, regions that included the infarcted tissue were not used for analysis. In some patients, only a few of the seven MCA regions were used. The present technique with contiguous regions preserved more regional data for analysis. In addition, this method easily accommodates the use of co-registered MR images for identifying and excluding regions of tissue infarction.

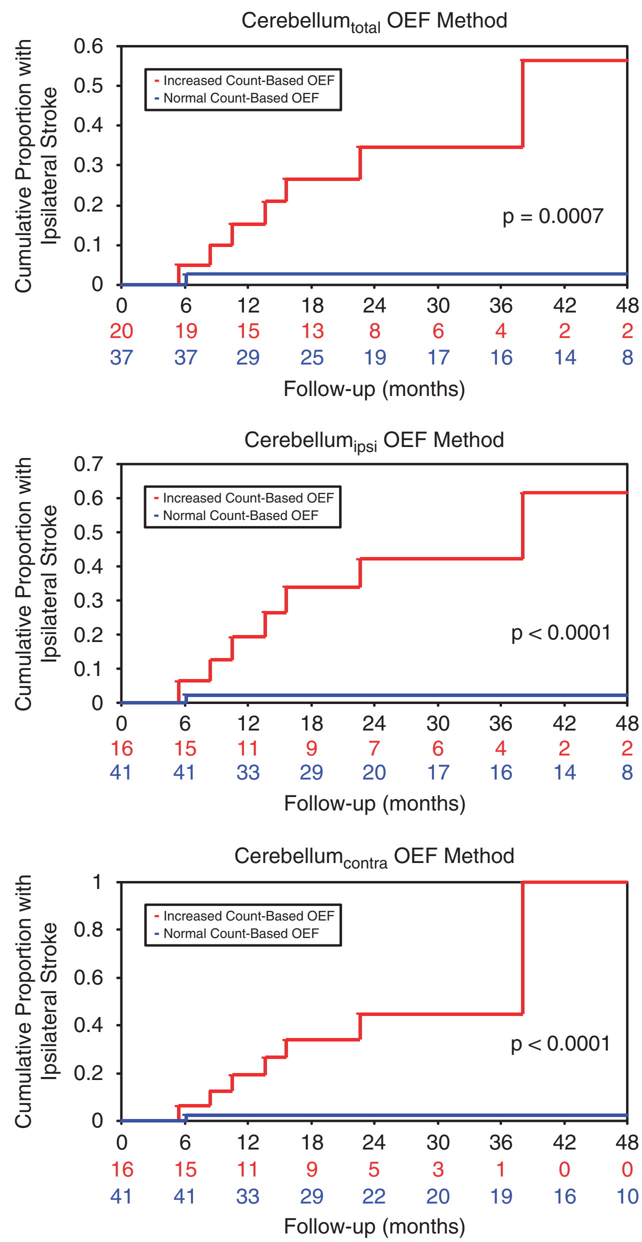

Figure 3 Kaplan–Meier cumulative failure curves for the end point of ipsilateral stroke for 57 patients with symptomatic carotid occlusion who were examined by using the three count-based cerebellar OEF methods. In each case, one stroke occurred in patients with normal count-based OEF (cbOEF) (blue), and the other seven strokes occurred in patients with elevated cbOEF (red). The number of patients remaining event free and available for follow-up evaluation at each 6-month interval is shown at the bottom of the graph. Abbreviation: OEF, oxygen extraction fraction.

We explored the use of regions other than the cerebellum, such as the posterior cerebral artery (PCA) territory. One problem with using the PCA territory in our current data set was the limited angiography data available on these patients. The PCA territory may have been supplied by the carotid in some patients. Angiographic images were reviewed on study entry, but were not stored and the origin of the PCA was not recorded. The second, and more important, problem was the small volume of the core PCA territory (van der Zwan *et al*, 1992) and the proximity to the straight sinus and torcula. These structures have extremely high counts on the cbOEF images, owing to the lack of a correction for CBV (Figure 1). The presence of large venous sinuses is also an issue in the posterior fossa, but the cerebellar regions are larger than the PCA territory. To minimize the effect of structures with large counts on adjacent lower count regions (partial-volume averaging), we used a 10-mm filter for the cbOEF images, rather than the 16-mm filter we have used in the past.

Other investigators have used the cerebellum as a reference normal for the cerebral hemispheres, but have not validated this technique as a predictor of stroke risk. Ibaraki *et al* (2004) presented a method for relative measurement of CBF, OEF, and metabolic rate of oxygen ($CMRO_2$) using PET without arterial sampling in patients with hyperacute ischemic stroke. For relative CBF, OEF, and $CMRO_2$, ipsilateral cerebellum was used as the reference region. Data obtained using this semiquantitative PET method was compared with the quantitative PET data for six patients and the differences between the two methods were found to be relatively insignificant. Imaizumi *et al* (2002) examined the use of single-photon emission computed tomography (SPECT) with an acetazolamide challenge to screen patients with carotid occlusive disease for misery perfusion. Their aim was to clarify the relationship between cerebrovascular reserve and CBF measured semi-quantitatively with SPECT and OEF measured quantitatively with PET. Because of the inclusion of five patients with bilateral disease, cerebellum was used as a control region for the semiquantitative SPECT. Although neither cerebrovascular reserve nor CBF alone was useful for detecting lesions with elevated OEF, the combination of the two provided an index with high sensitivity, specificity, and positive predictive value for the detection of misery perfusion. Tanaka *et al* (2006) used data from moyamoya patients to analyze whether the hemodynamic parameters obtained with perfusion-weighted MRI (PWI) were reliable for use in clinical decision-making. They used cerebellum as the control region and concluded that PWI provided adequate quantitative evaluations of CBV and mean transit time, but not CBF, in moyamoya patients.

One potential limitation of using cerebellum as the control for a cbOEF method is the issue of CCD. This term refers to hypometabolism in a cerebellar hemisphere contralateral to a cerebral hemispheric infarction (Feeney and Baron, 1986; Pantano *et al*, 1986; Yamauchi *et al*, 1992). This phenomenon presumably arises due to a disconnection of cerebro-ponto-cerebellar pathways, causing a reduction in metabolism and subsequently oxygen utilization (Pantano *et al*, 1986; Yamauchi *et al*, 1992). CBF decreases in response to the reduced metabolic demand.

There are conflicting data regarding the relative reduction in CBF and the reduction in $CMRO_2$. Baron *et al* (1993) and Pantano *et al* (1986) found matched reductions in CBF and $CMRO_2$. Yamauchi *et al* (1992) found slightly greater reductions in CBF relative to $CMRO_2$, leading to a slight increase in OEF in the cerebellar hemisphere contralateral to the infarction relative to the ipsilateral cerebellar hemisphere. Similarly, Martin and Raichle (1983) studied 10 patients with frontal lobe infarctions and found a 19.7% mean reduction in CBF and a 16.8% mean reduction in $CMRO_2$ in the contralateral versus the ipsilateral cerebellar hemisphere. We observed a trend towards higher cbOEF values in the contralateral cerebellar hemisphere in the 14 patients with CCD. This was not statistically significant as a group

Table 2 Changes in cbOEF status for patients using each method ($n = 57$), as compared with the MCA_{sphere} categorization

	Switch from normal to abnormal		*Switch from abnormal to normal*	
	Stroke	*No stroke*	*Stroke*	*No stroke*
MCA_{core}	0	4	0	4
$Cerebellum_{total}$	0	3	0	10
$Cerebellum_{ipsi}$	0	1	0	12
$Cerebellum_{contra}$	0	3	0	14

Abbreviations: cbOEF, count-based oxygen extraction fraction; MCA, middle cerebral artery.

Table 3 Diaschisis subgroup: analysis of cbCBF and cbOEF in patients with and without diaschisis

		Contra/Ipsi cerebellum cbCBF ratio			*Contra/ipsi cerebellum cbOEF ratio*		
	N	*Mean*	*s.d.*	*95% CL*	*Mean*	*s.d.*	*95% CL*
Normal range[a]	13	1.008	0.022	0.959–1.056	0.980	0.044	0.883, 1.076
No diaschisis	43	1.004	0.043	0.911, 1.097	0.995	0.047	0.895, 1.096
Diaschisis	14	0.910	0.038	0.828, 0.992	1.020	0.052	0.908, 1.132

Abbreviations: cbCBF, count-based cerebral blood flow; cbOEF, count-based oxygen extraction fraction; CL, confidence limit.
[a]The left/right ratios of cbCBF and cbOEF.

Table 4 Baseline risk factors in CCD versus non-CCD

	CCD (n = *14*)	*non-CCD* (n = *43*)	*Total* (n = *57*)	P
Age, years (mean ± s.d.)	63 ± 6.8	64 ± 9.3	64 ± 8.7	0.71
Sex				
Male	8 (57%)	28 (65%)	36 (63%)	0.75
Female	6 (43%)	15 (35%)	21 (37%)	
Cerebrovascular history				
Cerebral TIA	2 (14%)	13 (30%)	15 (26%)	0.08
Cerebral stroke	12 (86%)	21 (49%)	33 (58%)	
Retinal TIA	0	8 (19%)	8 (14%)	
Retinal stroke	0	1 (2%)	1 (2%)	
Hypertension	7 (50%)	26 (60%)	33 (58%)	0.54
Prior myocardial infarction	2 (14%)	11 (26%)	13 (23%)	0.48
Diabetes mellitus	2 (14%)	13 (30%)	15 (26%)	0.31
Smoking				
Never	2 (14%)	5 (12%)	7 (12%)	0.04
Ex-smoker	2 (14%)	21 (49%)	23 (40%)	
Current smoker	10 (71%)	17 (40%)	27 (47%)	
Alcohol consumption				
None	10 (71%)	31 (72%)	41 (72%)	1
Drinkers, drinks/week (mean ± s.d.)	35 ± 35	25 ± 34	28 ± 34	0.35
Parental death from stroke	3 (23%)	10 (24%)	13 (24%)	1
Laboratory				
Hemoglobin, g/dL (mean ± s.d.)	12.1 ± 1.5	12.6 ± 1.3	12.5 ± 1.4	0.25
Fibrinogen, mg/dL (mean ± s.d.)	388 ± 75	378 ± 91	380 ± 86	0.71
Cholesterol				
HDL, mg/dL (mean ± s.d.)	42.5 ± 12.0	42.5 ± 12.8	42.5 ± 12.5	1
LDL, mg/dL (mean ± s.d.)	153.5 ± 31.7	139.3 ± 37.2	142.7 ± 36.2	0.24
Triglycerides, mg/dL (mean ± s.d.)	190.3 ± 69.8	221 ± 187.8	214 ± 168.3	0.58
Contralateral stenosis				
< 50%	10 (77%)	28 (87.5%)	38 (84%)	0.39
> 50%	3 (23%)	4 (12.5%)	7 (16%)	

Abbreviations: CCD, crossed cerebellar diaschisis; HDL, high-density lipoprotein; LDL, low-density lipoprotein; TIA, transient ischemic attack.

and did not affect the categorization of patients with stroke during follow-up. Nevertheless, this phenomenon might account for the slightly lower r^2 value in the linear regression analysis of the cerebellum$_{contra}$ method. These data suggest that the performance of the cerebellum as the reference normal in patients with unilateral or bilateral strokes will be affected by CCD, and that this effect will be minimal.

The methodology we used to define the presence of CCD was different from that used in earlier studies. Earlier studies have used absolute measurements of CBF in the cerebellum and cerebral hemispheres (Feeney and Baron, 1986; Pantano *et al*, 1986; Yamauchi *et al*, 1992, 1994) to define CCD. We used left-to-right (or right-to-left, depending on the side of the occluded artery) ratios of the counts from the O-15 water study. These ratios are an accurate measurement of relative CBF (Raichle *et al*, 1983). We considered patients with reduced CBF in the cerebellar hemisphere contralateral to an occluded carotid artery to have CCD if the reduction was outside of the normal range of left/right CBF ratios. This categorization may have been slightly changed if other criteria were used. The point of this analysis was to investigate whether CCD adversely affected the ability of cerebral-to-cerebellar cbOEF ratios to identify patients at high risk for stroke. We found no evidence for this to be the case. All four patients with reduced contralateral cerebellar CBF beyond the normal range of cerebellar asymmetry (presumed CCD) that suffered a stroke on follow-up were categorized as having increased OEF by each of the three hemisphere to cerebellar cbOEF ratios.

The patients with CCD in this study were more likely to have had a prior stroke than those without CCD. Two of the CCD patients were not categorized as having had a stroke (transient ischemic attack). Given the strong association between stroke and CCD, it is likely that these patients had tissue infarction but a clinical transient ischemic attack (Easton *et al*, 2009; Kidwell *et al*, 1999). Baseline imaging in STLCOS was generally a noncontrast computed tomography scan. Stroke location was not recorded on study entry. These images were not stored and were not available for review in this study. We also observed a trend between current smoking and CCD. This may be related to the association between smoking and stroke risk rather than CCD.

The methodology used for the measurement of cerebellar counts could be improved and standardized. We observed a significant variability in the size, location, and intensity of the venous sinuses surrounding the cerebellum in our 57 patients. The atlas-based stereotactic cerebellar regions commonly included these structures, necessitating hand-drawn regions. Using Gaussian filtering smoothes the PET images and aids in visual interpretation, but also contributes to partial-volume averaging of the high-signal venous sinuses into the adjacent tissue. The use of unfiltered PET images may reduce the impact of this problem. Another approach might involve automated thresholding of these high-count structures.

We assumed that the cerebellar OEF was normal, except for the effects of diaschisis. It is possible that some of these patients had increased OEF in one or both cerebellar hemispheres owing to atherosclerotic occlusive disease of the posterior circulation. The entry requirements for the STLCOS required carotid imaging to confirm occlusion, but no vascular imaging for the posterior circulation was required or recorded. However, the patients in the STLCOS were required to have ischemic symptoms referable to the occluded carotid artery. Any posterior circulation atherosclerotic disease was asymptomatic, therefore, and was unlikely to be associated with increased OEF based on this fact alone (Powers *et al*, 2000).

Two different PET scanners were used over the course of this study. These scanners had slightly different FOVs and in-plane resolution. It is unlikely that these factors had any impact on the regional measurements obtained in this study. The 953B scanner acquires 31 slices with 3.375 mm slice separation, 10 cm axial FOV, with transaxial and axial resolutions of about 5 mm full-width at half-maximum. The EXACT HR acquires 47 slices with 3.125 mm separation, 15 cm axial FOV, with transaxial and axial resolutions of just <4 mm. All scans in the current study were acquired in 2D mode (septa extended) and were reconstructed using measured attenuation and scatter correction. With the 2D mode, relative sensitivity drops for only four end planes on the HR scanner and for three on the 953B scanner. All primary images used in data analysis were Gaussian filtered to 3D resolutions of 16 mm full-width at half-maximum (using kernels defined separately for each scanner and for axial versus transaxial dimensions). At this reduced resolution, slight differences in intrinsic resolution and axial sampling become irrelevant for subsequent analysis. Both scanners have been tested for accuracy (i.e., 3D spatial uniformity) using offset cylindrical phantoms, and there was no bias in any of the axial planes. With images from either scanner, volume of interests were not to be defined in the end planes; however, this was motivated by noise considerations rather than accuracy. Moreover, cerebellar volumes of interest were large (60 mL) relative to both voxel and slice size. Finally, when the EXACT HR was being considered as a replacement for the 953B scanner in ongoing studies, scans were acquired using the Hoffman 3D brain phantom on both scanners. These were reconstructed and filtered in the same manner as used in this study and then co-registered and normalized. Images from one scanner were compared with those from the other scanner directly using subtraction imaging, and there were no detectable differences.

One final potential limitation of this analysis is that this validation study was performed in a group of patients with unilateral carotid occlusion. It is possible, although unlikely, that MCA-to-cerebellar ratios would not correlate as well in patients with bilateral occlusions. Only seven patients in the current cohort had contralateral atherosclerotic disease $>50\%$. The cerebellar ratio method seemed to perform similarly in this group of seven patients. An ideal analysis would test the ability of this method to predict the outcome in a population of patients with bilateral carotid occlusive disease, such as the moyamoya phenomenon.

In summary, we have demonstrated that the cerebellum may be used as the reference for normal for the detection of increased cerebral cbOEF in patients with atherosclerotic carotid occlusion. The effects of diaschisis are minimal, and can be corrected for if unilateral. This method has great potential for the detection of increased cbOEF in patients with bilateral occlusive processes, such as the moyamoya phenomenon (Hallemeier *et al*, 2006). Further prospective studies will be necessary to determine whether these measurements of hemodynamic compromise are predictive of the risk of subsequent stroke.

Conflict of interest

The authors declare no conflict of interest.

References

Baron JC, Bousser MG, Rey A, Guillard A, Comar D, Castaigne P (1981) Reversal of focal 'misery perfusion syndrome' by extra-intracranial artery bypass in hemodynamic cerebral ischemia. A case study with 0-15 positron emission tomography. *Stroke* 12:454–9

Baron JC, Marchal G, Serrati C, Rioux P (1993) Crossed cerebellar diaschisis: further pathophysiological investigations with PET in the acute and subacute stage of MCA territory infarction. *J Cereb Blood Flow Metab* 13:S275

Derdeyn CP, Videen TO, Grubb Jr RL, Powers WJ (2001) Comparison of PET oxygen extraction fraction methods for the prediction of stroke risk. *J Nucl Med* 42:1195–7
Derdeyn CP, Videen TO, Simmons NR, Yundt KD, Fritsch SM, Grubb Jr RL, Powers WJ (1999) Count-based PET method for predicting ischemic stroke in patients with symptomatic carotid arterial occlusion. *Radiology* 212:499–506
Derdeyn CP, Videen TO, Yundt KD, Fritsch SM, Carpenter DA, Grubb RL, Powers WJ (2002) Variability of cerebral blood volume and oxygen extraction: stages of cerebral haemodynamic impairment revisited. *Brain* 125:595–607
Derdeyn CP, Yundt KD, Videen TO, Carpenter DA, Grubb Jr RL, Powers WJ (1998) Increased oxygen extraction fraction is associated with prior ischemic events in patients with carotid occlusion. *Stroke* 29:754–8
Easton JD, Saver JL, Albers GW, Alberts MJ, Chaturvedi S, Feldmann E, Hatsukami TS, Higashida RT, Johnston SC, Kidwell CS, Lutsep HL, Miller E, Sacco RL (2009) Definition and evaluation of transient ischemic attack: a scientific statement for healthcare professionals from the American Heart Association/American Stroke Association Stroke Council; Council on Cardiovascular Surgery and Anesthesia; Council on Cardiovascular Radiology and Intervention; Council on Cardiovascular Nursing; and the Interdisciplinary Council on Peripheral Vascular Disease: the American Academy of Neurology affirms the value of this statement as an educational tool for neurologists. *Stroke* 40:2276–93
Feeney DM, Baron JC (1986) Diaschisis. *Stroke* 17:817–30
Fox PT, Perlmutter JS, Raichle ME (1985) A stereotactic method of anatomical localization for positron emission tomography. *J Comput Assist Tomogr* 9:141–53
Frackowiak RSJ, Lenzi G-L, Jones T, Heather JD (1980) Quantitative measurement of regional cerebral blood flow and oxygen metabolism in man using O-15 and positron emission tomography: theory, procedure, and normal values. *J Comput Assist Tomogr* 4:727–36
Grubb Jr RL, Derdeyn CP, Fritsch SM, Carpenter DA, Yundt KD, Videen TO, Spitznagel EL, Powers WJ (1998) Importance of hemodynamic factors in the prognosis of symptomatic carotid occlusion. *JAMA* 280:1055–60
Hallemeier CL, Rich KM, Grubb Jr RL, Chicoine MR, Moran CJ, Cross 3rd DT, Zipfel GJ, Dacey Jr RG, Derdeyn CP (2006) Clinical features and outcome in North American adults with moyamoya phenomenon. *Stroke* 37:1490–6
Ibaraki M, Shimosegawa E, Miura S, Takahashi K, Ito H, Kanno I, Hatazawa J (2004) PET measurements of CBF, OEF, and CMRO2 without arterial sampling in hyperacute ischemic stroke: method and error analysis. *Ann Nucl Med* 18:35–44
Imaizumi M, Kitagawa K, Hashikawa K, Oku N, Teratani T, Takasawa M, Yoshikawa T, Rishu P, Ohtsuki T, Hori M, Matsumoto M, Nishimura T (2002) Detection of misery perfusion with split-dose 123I-iodoamphetamine single-photon emission computed tomography in patients with carotid occlusive diseases. *Stroke* 33:2217–23
Jones T, Chesler DA, Ter-Pogossian MM (1976) The continuous inhalation of Oxygen-15 for assessing regional oxygen extraction in the brain of man. *Br J Radiol* 49:339–43
Kidwell CS, Alger JR, Di Salle F, Starkman S, Villablanca P, Bentson J, Saver JL (1999) Diffusion MRI in patients with transient ischemic attacks. *Stroke* 30:1174–80
Kobayashi M, Okazawa H, Tsuchida T, Kawai K, Fujibayashi Y, Yonekura Y (2006) Diagnosis of misery perfusion using noninvasive 15O-gas PET. *J Nucl Med* 47:1581–6
Martin WR, Raichle ME (1983) Cerebellar blood flow and metabolism in cerebral hemisphere infarction. *Ann Neurol* 14:168–76
Mintun MA, Raichle ME, Martin WRW, Herscovitch P (1984) Brain oxygen utilization measured with O-15 radiotracers and positron emission tomography. *J Nucl Med* 25:177–87
Pantano P, Baron JC, Samson Y, Bousser MG, Derouesne C, Comar D (1986) Crossed cerebellar diaschisis. Further studies. *Brain* 109:677–94
Powers WJ, Derdeyn CP, Fritsch SM, Carpenter DA, Yundt KD, Videen TO, Grubb Jr RL (2000) Benign prognosis of never-symptomatic carotid occlusion. *Neurology* 54:878–82
Raichle ME, Martin WR, Herscovitch P, Mintun MA, Markham J (1983) Brain blood flow measured with intravenous H2(15)O.II. Implementation and validation. *J Nucl Med* 24:790–8
Talairach J, Tournoux P (1988) *Co-Planar Stereotactic Atlas of the Human Brain*. New York: Thieme Medical Publishers
Tanaka Y, Nariai T, Nagaoka T, Akimoto H, Ishiwata K, Ishii K, Matsushima Y, Ohno K (2006) Quantitative evaluation of cerebral hemodynamics in patients with moyamoya disease by dynamic susceptibility contrast magnetic resonance imaging–comparison with positron emission tomography. *J Cereb Blood Flow Metab* 26:291–300
van der Zwan A, Hillen B, Tulleken CAF, Dujovny M, Dragovic L (1992) Variability of the territories of the major cerebral arteries. *J Neurosurg* 77:927–40
Welch MJ, Lifton JF, Ter-Pogossian MM (1969) The preparation of millicurie quantities of oxygen-15 labeled water. *J Lab Comp* 5:168–72
Welch MJ, Ter-Pogossian MM (1968) Preparation of short half-lived radioactive gases for medical studies. *Radiat Res* 36:580–7
Woods RP, Cherry SR, Mazziotta JC (1992) Rapid automated algorithm for aligning and reslicing PET images. *J Comput Assist Tomogr* 16:620–33
Woods RP, Grafton ST, Holmes CJ, Cherry SR, Mazziotta JC (1998) Automated image registration: I. General methods and intrasubject, intramodality validation. *J Comput Assist Tomogr* 22:139–52
Yamauchi H, Fukuyama H, Kimura J (1992) Hemodynamic and metabolic changes in crossed cerebellar diaschisis. *Stroke* 23:855–60
Yamauchi H, Fukuyama H, Kimura J, Ishikawa M, Kikuchi H (1994) Crossed cerebellar hypoperfusion indicates the degree of uncoupling between blood flow and metabolism in major cerebral arterial occlusion. *Stroke* 25: 1945–51
Yamauchi H, Fukuyama H, Nagahama Y, Nabatame H, Ueno M, Nishizawa S, Konishi J, Shio H (1999) Significance of increased oxygen extraction fraction in five-year prognosis of major cerebral arterial occlusive disease. *J Nucl Med* 40:1992–8